# Absolute Total Cross Sections for the Scattering of Low-Energy Electrons by Rubidium, Cesium, and Potassium*†

Paul J. Visconti, James A. Slevin,‡ and Kenneth Rubin
*City College of the City University of New York, New York, New York* 10031
(Received 7 May 1970)

Using the atom-beam recoil technique, absolute total cross sections were measured for the scattering of electrons in the energy range 0.3–9 eV by potassium, rubidium, and cesium. The results of these measurements are in substantial disagreement with the experimental values of Brode, obtained more than 40 years ago. On the other hand, our potassium cross sections agree extremely well with the recent calculations of Karule, and Karule and Peterkop, as well as with the experimental values of Collins *et al.* For cesium and rubidium, the existing theoretical calculations are not in as good agreement with our results as in the case of potassium.

## I. INTRODUCTION

Of late there has been evidence, both experimental and theoretical, that the heretofore accepted low-energy electron-alkali total cross sections may be in error, both in magnitude and variation with energy. Essentially, all the aforementioned total-cross-section data contained in the literature were obtained by Brode[1] more than 40 yr ago, using a modified Ramsauer-type apparatus.[2] A number of recent calculations,[3–7] however, give results that differ significantly from Brode's values. In addition, absolute potassium data, obtained by Collins *et al.*,[8] with a quoted accuracy of 20%, differs from Brode's values by a factor of 2. Furthermore, Perel *et al.*[9] made some measurements of the ratio of the Li to K cross sections which, if normalized to Collin's data,[10] give better agreement with theoretical calculations of the Li cross sections than do Brode's values. While there is no guarantee that any of these calculations are correct, the excellent agreement between Collin's data and the calculations of Karule[3] and Karule and Peterkop[4] make the rest of Brode's results suspect. It is possible that Brode's data may be incorrect for the following reasons:

(i) Electron energy selection and collisions with the vapor under study were not, in Brode's system, performed in separate chambers. Therefore, the filament of his electron gun was continuously exposed to an atmosphere of hot alkali vapor. Such exposure could result in a significant lowering of the emitter's work function. Because of this, the implicit assumption by Brode that his electron velocity distribution remained constant for different vapor densities may be incorrect.

(ii) There are uncertainties, indicated by Brode himself,[1] in the determination of the true vapor density of the element under study.

For the above-mentioned reasons, we felt that it was desirable to perform a series of precision, absolute total-cross-section measurements on several of the alkalies.

## II. EXPERIMENTAL METHOD

The data presented here were obtained by using the atom-beam recoil technique. Essentially, this is a crossed-beam experiment with observation made on the scattered atoms. This technique has been described in detail elsewhere.[11] Figure 1 is a schematic diagram of the apparatus. We discuss the various components below.

### A. Atom Detection System

The atoms are detected by the usual combination of surface ionization detector and electron multiplier. The detector is 0.010 in. wide, and the half-width of the atom-beam profile in the plane of the detector is approximately 0.013 in.

### B. Electron Gun

The electron gun is a plane-parallel multigrid structure as shown in Fig. 2. The atom beam is intersected by the electrons in an equipotential region formed by two 0.250-in.-long molybdenum blocks and the grid $G_3$. Grids $G_1$ and $G_2$ serve to control the electron current and to some extent the velocity distribution of the electrons. A magnetic field of about 1200 G focuses the electrons. The collector plate $P_1$ has a small hole to permit a fraction of the electrons collected to pass through to the plate $P_2$. The plate $P_2$ is used in the retarding potential difference (RPD) measurements. Various masks serve to form an electron beam that is 0.057 in. high and 1 in. wide. The gun typically operates with currents between 30 and 110 $\mu$A and has an energy spread of less than 0.25 V, full width at half-maximum (FWHM) as determined from the RPD measurements.

### C. Velocity Selector

During one phase of the experiment it was necessary to use a velocity selected atom beam. The velocity selection was accomplished through the

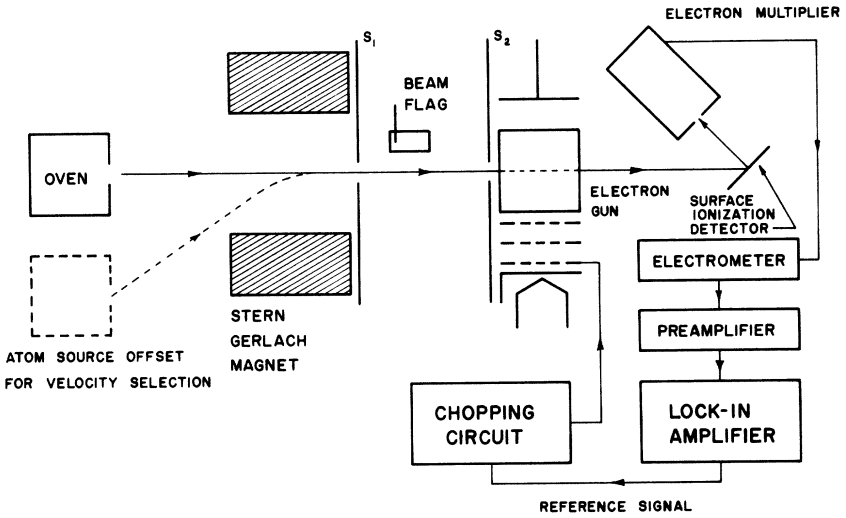


FIG. 1. Schematic of the apparatus including a block diagram of the detection system.

use of a Stern-Gerlach-type magnetic velocity filter. This consists of the inhomogeneous magnet and the two collimating slits $s_1$ and $s_2$ shown in Fig. 1. In operation, the oven is offset from the axis of the magnet and slits. Under this arrangement, only atoms having velocities within a small range of values $\Delta V$ about some value $V_0$ can pass from the oven and on through the slits. $\Delta V/V_0$ is deter-

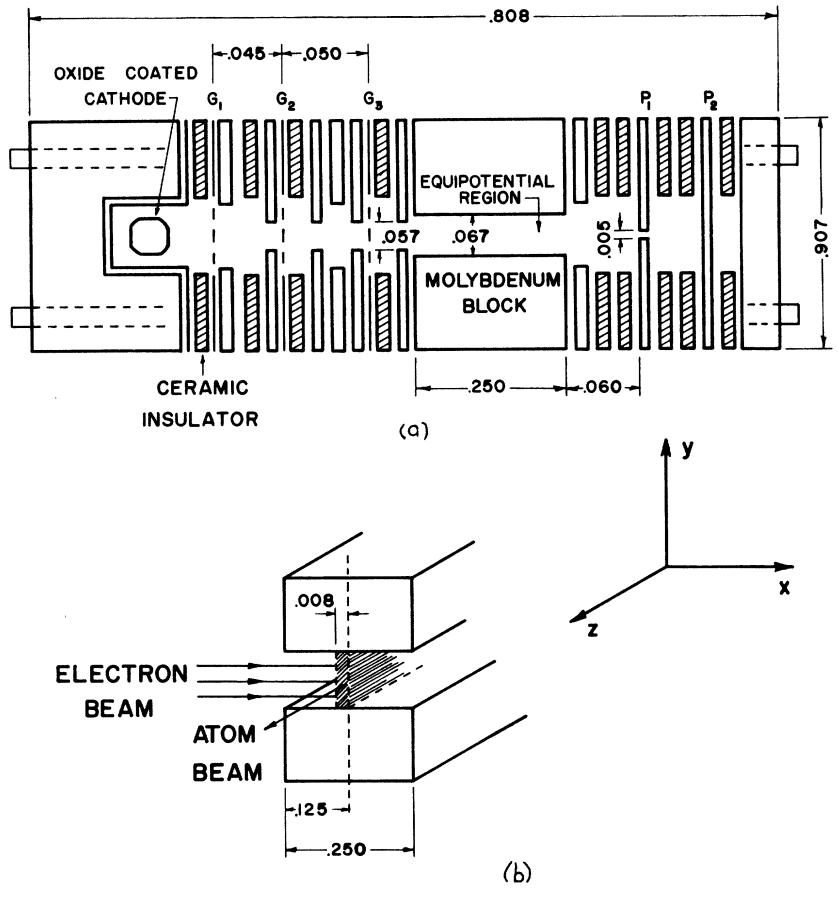


FIG. 2. (a) Schematic of the electron gun design; (b) scattering or interaction region.

mined by the slit widths and the amount of oven offset. The theory of this type of velocity selector is fully discussed in Ref. 12.

### D. Detection of Scattering Signals

Phase-sensitive detection methods are used to detect the scattering signals. When the detector is placed on the axis of the atom beam, scattering events cause the detector signal to decrease by a small amount. This decrease in detector signal will be referred to as the scattering out signal. Since the electron gun is modulated, this scattering signal is ac and is detected by standard phase-sensitive techniques. The ac signal represents a very small fraction of the full atom-beam current, of the order of one part in 1000. The full beam current is therefore a dc signal and will be referred to as the dc beam. If the detector is displaced far enough from the atom-beam axis in a direction parallel to the direction of motion of the electrons, it is possible to pick up the scattered atoms. This will again be an ac scattering signal but one which is 180° out of phase with the scattering out signal. We will refer to this signal as the differential or scattering in signal. Both the ac and dc detection systems are shown schematically in Fig. 1.

### E. Data-Acquisition System

An automated data-acquisition system was used to facilitate the accumulation of the data over protracted periods of time. In the majority of cases this reduced the error in the cross sections due to statistical fluctuations to less than 5%.

The data-acquisition system, shown in the block diagram in Fig. 3, employed an input scanner, a voltage to frequency converter, a preset counter, and an output coupler to an IBM keypunch. Nine separate voltages were automatically sequentially digitized, integrated, and recorded as nine 5-digit numbers on IBM cards. Each data run included an 80-sec integration of the scattering signal and 10-sec integrations of both the atom- and electron-beam currents. Five to ten runs were taken at each electron energy from which an average cross section was obtained together with an rms deviation.

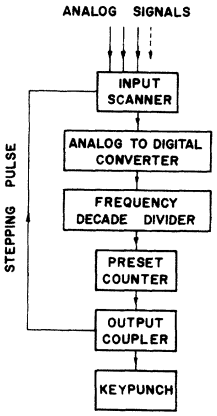


FIG. 3. Block diagram of the automatic data-acquisition system.

## III. SPECIAL CONSIDERATIONS IN EVALUATING POSSIBLE SOURCES OF SYSTEMATIC ERROR

### A. Evaluation of Experimental Cross Section

In an atom-beam-recoil experiment, the cross section $Q$ is related to the various experimental parameters by the expression

$$Q = (I_S/I_A)\,\bar{V}_e\,H/I_e\,, \tag{1}$$

where $I_S$ is the ac scattering current, $I_A$ the dc beam current, $H$ the height of the atom beam in the interaction region, $I_e$ the total electron current passing through the atom beam, $e$ the charge on the electron, and $\bar{V}$ an average atom velocity obtained from the expression

$$\frac{1}{\bar{V}} = \int \frac{1}{V} f(V)\,dV\,, \tag{2}$$

where $f(V)$ is the normalized velocity distribution of the atom-beam current. The problems involved in evaluating the various parameters in Eq. (1) are discussed in detail below.

#### 1. $H$

The expression for $Q$ in Eq. (1) assumes that the height of the atom beam is equal to or greater than that of the electron beam and that the atom current density is uniform over its height, while the electron current density is uniform over the length of the interaction region, measured in the direction of motion of the atoms. The value of $H$ is then determined by the separation of the two molybdenum blocks in Fig. 2. As a check on these assumptions, cross-section data were obtained with a second gun in which the height of the electron beam was greater than that of the atom beam. Here $H$ in Eq. (1) represents the height of the electron beam and it is assumed that the electron current density is uniform over the height of the electron beam. The cross sections obtained with the two guns agreed to within 5%.

#### 2. $I_S/I_A$

Since both the ac scattering signal and dc beam are detected by the same surface ionization detector, electron multiplier, and electrometer, the ratio $I_S/I_A$ is independent of the absolute detector efficiency of this system. All that is required is the ratio of the ac to dc output voltages of the electrometer. This of course assumes that the ac and dc detection efficiencies are equal. This was checked by noting that there was no change in the ratio as

the modulation frequency was varied. (The fact that the absolute efficiency of the atom detector is not required is one of the great advantages of the atom-beam-recoil technique in measuring absolute cross sections.) The ac output voltage of the electrometer was measured using a lock-in amplifier and it was therefore necessary to obtain an accurate calibration of its gain. It was also necessary to take into account the shape and duty cycle of the modulation pulse. All these factors were checked by obtaining some cross-section measurements using the lock-in amplifier to measure the gun current as well as the scattering signal. This eliminates the gain of the lock-in from the expression for $Q$. The values of $Q$ obtained by this method agreed with our other data to within 3% and we therefore assume that errors in calibration amount to less than 3%.

### 3. $I_e$

The electron current $I_e$ is the total current to the plates $P_1$ and $P_2$ shown in Fig. 2. This assumes that no electrons are reflected back into the scattering region. This was checked by looking for a differential scattering signal on the side of the atom beam opposite to that, toward which the electrons would normally scatter the atoms. A scattering signal here would be due mainly to reflected electrons passing back through the atom beam.[13] We refer to this type of scattering as back scattering. As long as sufficiently large voltages were applied to the gun collector plate, no back scattering signal was observed. It should be noted that we did observe such a signal with an electron gun that had a grid, maintained at the same potential as the interaction region, between the interaction region and the collector plate $P_1$. We assume that the signal was due to electrons striking the grid and reflecting back into the scattering region. If this back scattering signal is taken into account, the value of $Q$ obtained with this gun agrees well with the values obtained with guns not containing such a grid.

### 4. $\bar{V}$

Probably the most uncertain quantity in the expression for $Q$ is $\bar{V}$. If the velocity distribution of the atom-beam current is known, $\bar{V}$ can be determined from Eq. (2). For example, if the beam is due to diffusion from a slit, then the velocity distribution in the beam flux is given by

$$f(V) = kVf_0(V)\,, \tag{3}$$

where $k$ is the normalization constant and $f_0(V)$ is the normalized velocity distribution in the oven. Since both $f(V)$ and $f_0(V)$ are normalized, $k = 1/\bar{V}_0$, where $\bar{V}_0$ is the average atom velocity in the oven. Equation (2) then gives a value of $\bar{V}$ which is equal to $\bar{V}_0$.

If then, we can assume that our atom beam does in fact correspond to that due to diffusion from a slit, we can determine $\bar{V}$ from the oven temperature. To check that this was indeed the case and that our thermocouples were giving us the true gas temperature, we obtained some values for $Q$ with a velocity selected atom beam. The beam was velocity selected using the magnetic velocity selector described in Sec. II and had a spread in velocities $\Delta V$ of about 0.2 V. A direct measurement was then made of the atom velocity as described below.

The details of the following argument are thoroughly covered in Ref. 11.

Basically, it can be shown that if observations are made of the differential scattering signal as a function of detector displacement at energies above the threshold for excitation, a peak will occur in the signal which is due to atoms having undergone an excitation by forward scattered electrons. The appearance of this peak is due to both the kinematics of the collision and the fact that the differential cross section is sharply peaked in the forward direction. The distance $Z$ between the peak of the dc beam and the peak in the differential scattering signal is given by

$$Z = L(2em)^{1/2}\left[1 - \left(1 - \frac{E_x}{E}\right)^{1/2}\right] \Big/ MV\,, \tag{4}$$

where $E$ is the electron energy, $E_x$ is the excitation energy, $V$ is the atomic velocity, $M$ is the atomic mass, $m$ is the electron mass, $e$ is the electron charge, and $L$ is the distance from the detector to the interaction region. Equation (4) can now be solved for the atom velocity $V$. The accuracy with which $V$ can be determined is dependent upon two quantities, $Z$ and $E$. It is possible to determine $Z$ to within $\pm 0.001$ in. The error in $E$, however, will depend upon the accuracy with which such quantities as contact potential and space charge corrections are known. For this reason, the determination of $V$ is carried out at a large enough electron energy to keep the error in $E$ small. In addition, the scattering peak is sharper at higher energies, since the velocity distribution in both the atom and electron beams tend to broaden the peak at low energies. At 30 V, we estimate the error in $E$ to be less than 1% and this leads to an error in $V$ of less than 6%. The cross sections obtained with the velocity selected atom beam agree with those obtained without velocity selection to within 5%.

In addition to yielding a value for the atom velocity, this method, above threshold, also provides a means of checking the electron-energy measurement made by retarding-potential techniques. Once the atom velocity is determined, the differential peaks can be located as a function of energy, in the

TABLE I. Comparison of absolute electron energies determined by the recoil technique with those obtained from retarding-potential measurements corrected for space charge.

| Equipotential-region voltage | Absolute electron-energy | |
|---|---|---|
| | Recoil method | RPD space charge calc |
| 9 V | 8 ± 0.15 eV | 7.9 ± 0.15 eV |
| 7 V | 6 ± 0.15 eV | 5.9 ± 0.15 eV |
| 4 V | 3 ± 0.15 eV | 2.9 ± 0.15 eV |

range of energies used in our cross-section measurements. Equation (4) can then be solved for $E$. It should be noted that the value of $E$ determined in this manner is the absolute value of the electron energy in the interaction region. We estimate that $E$ can be determined to within 0.15 eV. A comparison of the electron energies obtained as described above with those obtained from retarding-potential measurements together with space charge corrections is given in Table I.

### B. Resolution

As discussed in Sec. III A, we can determine, from the experimental parameters, a fairly precise value for the quantity $Q$ in Eq. (1). This value of $Q$ is the experimental value of the cross section and is not necessarily equal to the theoretical value.[14] The finite resolution of our apparatus will result in an experimental cross section that is always less than the theoretical value. The difference between the two values of the cross section is dependent upon both the resolution of the apparatus and the magnitude of the small-angle elastic scattering.[15] The resolution, in turn, is affected by two things; the distribution of the dc beam within the region of the detector, which determines the fraction of atoms scattered within this region that miss the detector, and the amount of dc beam to the left of the detector which determines the number of atoms scattered into the detector from those regions to its left (this assumes that the atoms are scattered from left to right). The resolution of the apparatus improves as the detector is moved to the left relative to the center of the dc beam. This improvement is due both to the increase in the fraction of the dc beam within the detector region lying closer to the right edge of the detector, and the decrease in the amount of dc beam lying to the left of the detector. If then, we observe the experimental cross section $Q$ as a function of detector position, its value should increase as the detector is moved to the left approaching, in the limit, the theoretical value. We can define an effective detector width $\Delta X$ which is a weighted average of the distribution of the dc beam within the region of the detector.[16] This effective width decreases as the detector is moved to the left. Assuming that the detector is in such a position that no dc beam lies to its left and in addition that the differential cross section is constant over the range of electron-scattering angles corresponding to $\Delta X$, it can be shown that the fractional difference between the experimental and theoretical cross section is given by

$$\frac{(Q_T - Q)}{Q_T} = \frac{MV}{(2emE)^{1/2}} \frac{2\pi\sigma(0)\Delta X}{Q_T L}, \tag{5}$$

where $\sigma(0)$ is the differential cross section at 0° and the other quantities are as defined previously. Equation (5) indicates that as the detector is moved to the left, $Q$ should increase linearly with decreasing $\Delta X$, approaching $Q_T$ as $\Delta X$ approaches zero. It should therefore be possible to obtain $Q_T$ by extrapolation of the curve of $Q$ vs $\Delta X$ and, in addition, $\sigma(0)$ from the slope of this curve. Unfortunately, as the detector is moved to the left, the scattering signal decreases, approaching zero as $\Delta X$ goes to zero, making it increasingly difficult to obtain reliable data. We present some preliminary results of the variation of $Q$ with $\Delta X$ for Rb in Fig. 4 and Cs in Fig. 5. The curves do indeed appear to be straight lines; however, the rather poor statistics prevent us from performing a good extrapolation. We are at the present time acquiring more data of

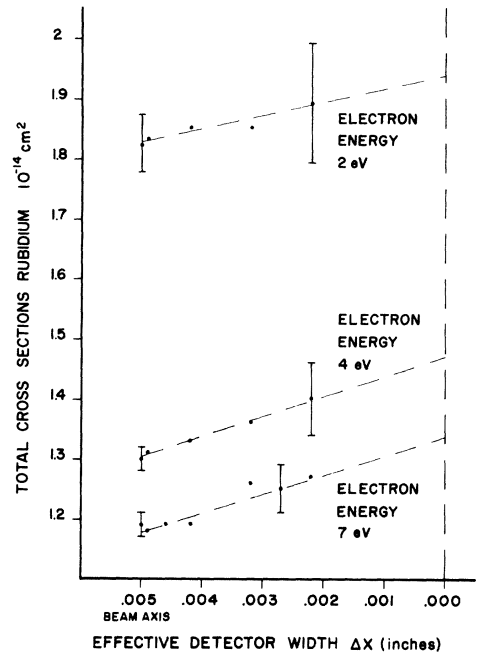


FIG. 4. Measured rubidium total cross sections vs effective detector width at electron energies 7, 4, and 2 eV. The atom-scattering signal is equal to zero for zero effective width.

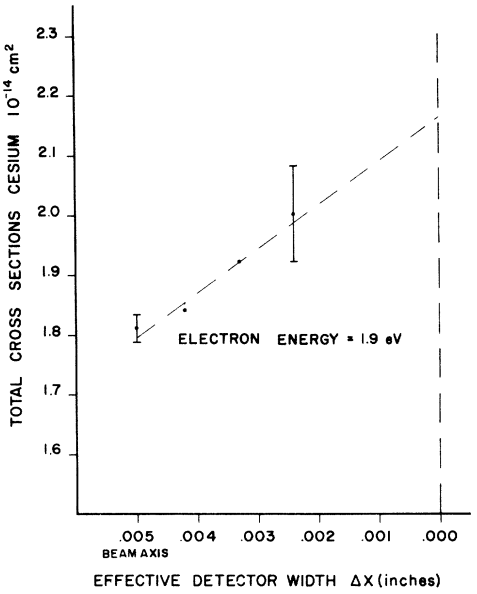


FIG. 5. Measured cesium total cross sections vs effective detector width at electron energy 1.9 eV. Atom-scattering signal is equal to zero for zero effective width.

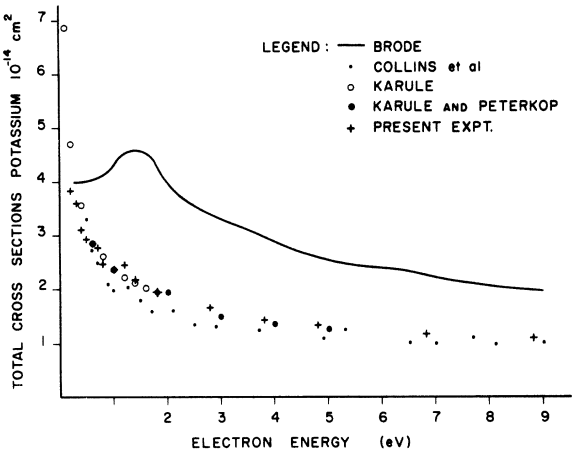


FIG. 6. Absolute total cross sections for the scattering of low-energy electrons by potassium. The present results are compared with the experimental data of Collins *et al.* and Brode and also with the calculations of Karule and Karule and Peterkop.

this type and will, in the near future, present these results.

The cross sections that we present in the present paper were obtained with the detector displaced 0.006 in. to the left of the dc beam center. In this position, there is no dc beam to the left of the detector and $\Delta X$ has the value 0.0026 in. The curves in Fig. 4 indicate that for Rb the percent difference between the theoretical and the experimental cross sections is 3.5% at 2 V and 5% at 7 V. For Cs, Fig. 5 indicates a 10% difference at 1.9 V.

In Table II, we present the range of electron-scattering angles $\Delta\theta$ corresponding to $\Delta X = 0.0026$ in. for various electron energies. It should be noted that while $\Delta X$ is just a function of the geometry of the apparatus, $\Delta\theta$ is also a function of the energy, decreasing as the energy increases. The appearance of the factor $1/\sqrt{E}$ in Eq. (5) reflects this fact. This does not, however, mean that the resolution of the apparatus necessarily improves as the energy increases since an increase in the factor $\sigma(0)/Q_T$ in Eq. (5) could offset the change in $\Delta\theta$.

TABLE II. Unresolved small-angle scattering for K, Rb, and Cs at several electron energies.

| Alkali | Electron energy (eV) | Effective electron resolution angle ($\Delta\theta$) |
|---|---|---|
| Potassium | 1 | 7.7° |
| | 3 | 5.8° |
| | 5 | 5.1° |
| Rubidium | 1 | 11.8° |
| | 3 | 9.9° |
| | 5 | 8.9° |
| Cesium | 1 | 15.1° |
| | 3 | 11.4° |
| | 5 | 10.1° |

## IV. RESULTS

To insure proper operation of all components of the system, various checks were made. The scattering signal was tested for linearity with atom-beam and electron-gun current. In the case of the electron current, the signal at a given voltage becomes nonlinear when the current exceeds some maximum value (for example 200 $\mu$A at 0.5 V).

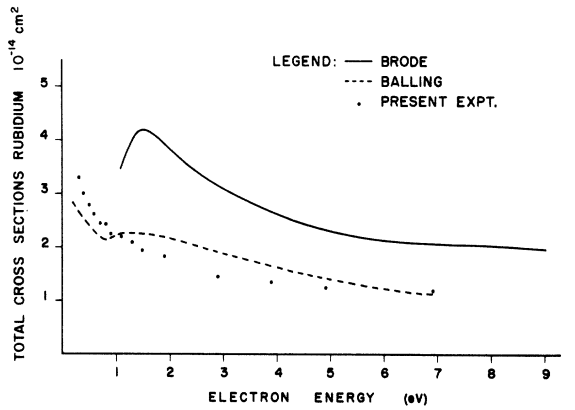


FIG. 7. Absolute total cross sections for the scattering of low-energy electrons by rubidium. Present results are compared with the experimental data of Brode and with the calculations of Balling.

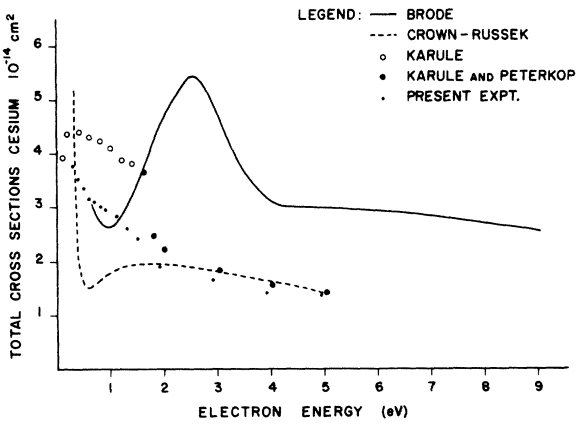


FIG. 8. Absolute total cross sections for the scattering of low-energy electrons by cesium. Present results are compared with the experimental data of Brode and also with the calculations of Crown and Russek, Karule, and Karule and Peterkop.

This nonlinearity is due to an appreciable alteration of the electron energy by the space charge in the electron beam. All cross-section data reported here were obtained in the linear region of the gun. A check was also made for field penetration into the scattering region from the gun collector, by varying the voltage on the collector and noting any change in the scattering signal. The signal was observed to remain constant as the voltage varied from 25 to 40 V above the interaction potential. Finally, the measured value of the atom-beam half-width agreed with the half-width calculated from the slit geometry to better than 5%. It is important to obtain this agreement since the effective detector width $\Delta X$ is calculated using the geometrical beam profile.

Electron energies and energy spread were obtained using retarding-potential measurements, with appropriate corrections made for space charge depression. The estimated error in the electron energy is ±0.15 eV with the energy spread above 2 eV less than 275 mV (FWHM) and below 2 eV less than 220 mV (FWHM).

The results of our total cross-section measurements are presented in Figs. 6–8. For all points shown, the statistical deviation of the data was less than ±6%. Each point represents a total integration time of approximately 10 min taken in intervals of 80 sec each.[17]

The systematic error was calculated to be less than ±9% based on an error of ±5% in $H$, ±5% in $I_s/I_A$, ±2% in $I_e$, and ±5% in $\overline{V}$. This gives an overall error in $Q$ of approximately ±10%. However, as discussed in Sec. III B, these values are expected to be less than the theoretical value due to the finite resolution of the apparatus. At this point we can only estimate the error due to resolution. In the case of potassium, we used Karule's phase shifts to calculate the small-angle scattering and found that there should be less than a 4% difference at 1.0 V between our measurements and Karule's calculations. This is consistent with the agreement we actually obtained. For Rb and Cs, we must rely on the measurements discussed in Sec. III B and presented in Figs. 4 and 5.

From the data we have obtained, we feel that the following conclusions can be made. In all cases, the substantial disagreement with Brode cannot be explained by any uncertainties in our experiment such as resolution, energy spread, statistics, etc. While it is true that the atom-beam-recoil technique, employed by both ourselves and Collins, is basically different from the modified Ramsauer technique used by Brode, both experiments if interpreted correctly should yield the same total cross-section values. Any large discrepancy can only be attributed to some significant systematic error in one or the other experiment. Since we believe that every possible source of major systematic error in our experiment has been checked and eliminated, we must conclude that Brode's results are incorrect.

The agreement between the $K$ calculations of Karule, Karule and Peterkop, and our data is well within our experimental error above 0.5 eV. Below 0.5 eV, $Q$ varies so rapidly with energy that any disagreement can probably be attributed to an uncertainty in our energy. In the case of Rb, the disagreement between our results and Balling's calculation is, at most energies, greater than the experimental error. We used Balling's phase shifts to calculate the small-angle scattering to see if in some cases this might explain the discrepancy (i.e., raise our values between 1.5 and 5 V), but the results are such that we cannot attribute our differences to resolution. Finally, for Cs, below about 1.5 eV, the disagreement with the calculations of Karule, Karule and Peterkop, and Crown and Russek are well outside the estimated accuracy of our experiment.

---

*Research supported by the National Science Foundation.

†From part of a thesis presented by Paul. J. Visconti in partial fulfilment of the requirements for the Ph. D. degree at the City University of New York.

‡Present Address: Stirling University, Stirling, Scotland.

[1]R. B. Brode, Phys. Rev. 34, 673 (1929).

[2]R. B. Brode, Proc. Roy. Soc. (London) A125, 134 (1929).

[3]E. M. Karule, JILA Information Center Report No. 3, University of Colorado, Boulder, Colo. (unpublished).

[4]E. M. Karule and R. K. Peterkop, JILA Information Center Report No. 3, University of Colorado, Boulder, Colo. (unpublished).
[5]J. C. Crown and A. Russek, Phys. Rev. 138, A669 (1965).
[6]L. C. Balling, Phys. Rev. 179, 78 (1969).
[7]P. Burke and J. Taylor, Technical Paper No. 367, Harwell, England, 1969 (unpublished).
[8]R. E. Collins, B. Bederson, and M. Goldstein, Phys. Rev. (unpublished).
[9]J. Perel, P. Englander, and B. Bederson, Phys. Rev. 128, 1148 (1962).
[10]In the Perel paper, the results were normalized to Brode's potassium cross sections.
[11]K. Rubin, B. Bederson, M. Goldstein, and R. E. Collins, Phys. Rev. 182, 201 (1969).
[12]B. Bederson and K. Rubin, Atomic Energy Commission, New York University, Technical Report No. NYO-10, 117, 1962 (unpublished).
[13]There is also the possibility of a signal here due to the action of the focusing magnetic field which causes the electrons to spiral in towards the atom beam. The electrons therefore strike the atoms in a small cone of angles about 90°. For the fields used, it can be shown that this effect is quite small.
[14]By theoretical value we mean here the integral of the differential cross section over all angles.
[15]As explained in Sec. III A, inelastically scattered atoms suffer deflections that are large compared to the dimensions of the detector and therefore need not be considered in the argument that follows.
[16]The expression for $\Delta X$ will be derived in a forthcoming paper that will treat the resolution problem at length.
[17]In the case of Rb, the data presented is the result of two curves taken at different times. Corresponding points on these curves agreed with each other to within the statistical deviation of the data.

PHYSICAL REVIEW A VOLUME 3, NUMBER 4 APRIL 1971

# Potential Curves for $He_2^+$ and $Li_2^+$

J. N. Bardsley
*University of Texas at Austin, Austin, Texas* 78712
*and Physics Department, University of Pittsburgh, Pittsburgh, Pennsylvania* 15213
(Received 25 May 1970)

*Ab initio* calculations are presented for several states of $He_2^+$ and $Li_2^+$ that are relevant to collision problems. In $He_2^+$, qualitative agreement is found with the predictions from the analysis of the oscillations and anomalous thresholds in $He^+$-He collision cross sections. For $Li_2^+$, the results suggest that the oscillations in $Li^+$-Li differential scattering cross sections are due to $\Sigma$-$\Pi$ transitions caused by the coupling of electronic and nuclear rotations.

## I. INTRODUCTION

The calculation of interatomic potential curves is an important part of the theory of atom-atom collisions. The techniques of computing the potential curves have been studied for many years by quantum chemists, and general methods and computer programs are now available for application to many systems. However, for the study of atomic collisions, a slight change of emphasis is required. For most collision problems it is preferable to calculate several potential curves to the same degree of accuracy rather than to concentrate all one's effort on a single curve. It is probably necessary to perform calculations in two steps: first, to obtain an over-all picture of the potential curves, and then to examine with more care the regions of nuclear separation of special interest.

The dependence of low-energy atomic collision cross sections on the interatomic potential curves has been discussed by many authors.[1,2] Of particular interest are the crossings of potential curves of states of different symmetry and the avoided crossings of curves belonging to states of the same symmetry. The importance of these crossings has been stressed by Lichten.[2] The basic hypothesis of low-energy collisions (in which nuclear motion is slow compared to electronic motion) is the adiabatic nature of the collision. During a collision of atoms $A$ and $B$, a particular electronic state of the molecule $AB$ is formed and a transition to another molecular state can only occur when the potential curves for the two states are very close together. Transitions between states thus occur mostly near crossings or avoided crossings.

This paper contains the results of calculations of potential curves for $He_2^+$ and $Li_2^+$. For $He_2^+$, the purpose was to obtain quantitative information concerning a well-known series of avoided crossings. For $Li_2^+$, the calculations were designed to discover the reason for the oscillations in the observed differential scattering cross sections.

## II. METHOD OF CALCULATION

The interatomic potentials were computed using the program VARY, written by Browne,[3] on the